Best Student Paper Award

A Computational Texture Masking Model for Natural Images Based on Adjacent Visual Channel Inhibition

Yucheng Liu and Jan P. Allebach

School of Electrical and Computer Engineering, Purdue University,
West Lafayette, IN 47906-2035, U.S.A.

ABSTRACT

Masking is a perceptual effect in which contents of the image reduce the ability of the observer to see the target signals hidden in the image. Characterization of masking effects plays an important role in modern image quality assessment (IQA) algorithms. In this work, we attribute the reduced sensitivity to the inhibition imposed by adjacent visual channels. In our model, each visual channel is excited by the contrast difference between the reference and distorted image in the corresponding channel and suppressed by the activities of the mask in adjacent channels. The model parameters are fitted to the results of a psychophysical experiment conducted with a set of different natural texture masks. Cross-validation is performed to demonstrate the model's performance in predicting the target detection threshold. The results of this work could be applied to improve the performance of current HVS-based IQA algorithms.

Keywords: image quality, contrast masking, defect visibility, natural image

1. INTRODUCTION

Masking is a perceptual effect in which the contents of the image inhibit the observer's ability to see a given target signal. For decades, researchers have been making significant efforts to understanding the nature of masking and trying to account for it in the modeling of the low level HVS.[1–7] Models for masking have been applied in many traditional image processing tasks, such as image compression,[8] digital watermarking,[9] image quality assessment (IQA).[2,10] With regard to IQA, the content of the image and the defects resulted from all aspects of image processing and rendering pipeline act as masks and targets, respectively. Mainstream perceptual IQA algorithms more or less account for the masking effect either explicitly in HVS models[6,7,11] or implicitly in non-HVS models.[10,12,13] Chandler[14] compares the performance of different IQA algorithms in predicting the local mask detection thresholds. Despite the success of many non-HVS based algorithms in evaluating overall image quality for natural images, HVS-based models demonstrate their superiority in predicting the detection threshold under natural masks. Among all mechanisms resulting in masking,[6,7] contrast masking receives the most discussion. Standard HVS models characterize contrast masking with a divisive gain control method that penalizes the visual response based on the contrast of the mask in the spatial neighborhood.[1,2,4] But the mechanism of gain control is still largely unknown and requires further research.

Despite the fact that considerable effort has been made to fit the model parameters to experimental data,[1,2,15] in most cases the parameters are only optimized for a very specific type of unnatural mask such as sinusoidal gratings or white noise. Very limited research has been devoted to investigating the masking phenomenon in natural image.[8,9,16,17] Masry[9] suggests reasonable masking prediction results for texture using a neural model[2] and parameters obtained from unnatural masks. Chandler[16] presents content-adaptive parameters for the same neural model using natural image masks and targets resulting from wavelet quantization. But the optimized parameters do not generalize well across different types of textures and defects.

Given the complexity of natural images and the neural response, we treat the neural-level activities of the HVS as a black box, and approach the masking effect by investigating the perceptual tolerance to a contrast difference in each visual channel. In this paper, we attribute the reduced sensitivity in one visual channel to the

Further author information: (Send correspondence to Yucheng Liu.)
Yucheng Liu: E-mail: yc-liu11@purdue.edu, Telephone: 1 765 421 5608
Jan P. Allebach: E-mail: allebach@purdue.edu, Telephone: 1 765 494 3535

Image Quality and System Performance XI, edited by Sophie Triantaphillidou, Mohamed-Chaker Larabi,
Proc. of SPIE-IS&T Electronic Imaging, SPIE Vol. 9016, 90160D · © 2014 SPIE-IS&T
CCC code: 0277-786X/14/$18 · doi: 10.1117/12.2038599

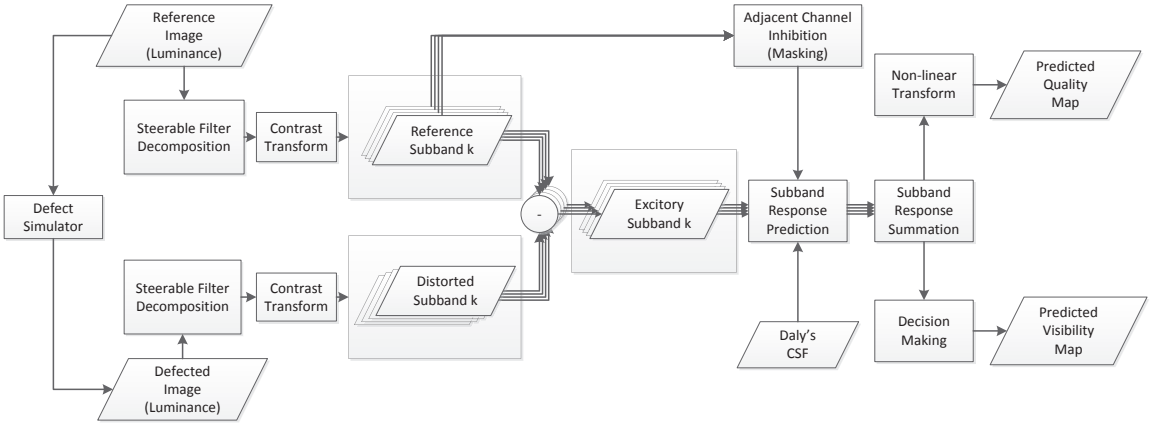

Figure 1. Flow diagram of the proposed visual model incorporating masking

activities of the mask in the adjacent channels. Results of psychophysical experiment are presented to support the validity of this model. Section 2 describes the masking model and parameters. Section 3 details the visual masking experiment using natural texture patches and discusses the results. In Sec. 4, we optimize the model parameters based on the experimental data and perform cross-validation to verify the effectiveness of the model. Finally, the conclusions are presented in Sec. 5.

2. MODEL DESCRIPTION

The flow diagram of the proposed model is given in Fig. 1. The reference image is processed through a defect simulator to generate an image with distortions that may result from a variety of image capture, processing, and rendering processes. The luminance channels of the reference image and distorted image are inputs to the framework that evaluates the perceptual difference. The first stage of the framework applies frequency-based decomposition to the image that simulates the multi-channel linear response of the HVS. Standard approaches at this stage include wavelet decomposition,[18] Gabor pyramid decomposition,[19] and specifically in this work, steerable pyramid decomposition.[5] After the decomposition stage, we follow Osberger's technique[4] and convert the sub-band decomposed image to a contrast map defined by Peli's Local Band-Limited Contrast:[20]

$$c_{k,o}(x,y) = \frac{a_{k,o}(x,y)}{l_k^*(x,y)}, \tag{1}$$

where $c_{k,o}$ is the local contrast of a particular frequency band at (k,o), where k and o indicate the radial frequency band and orientation, respectively (See Fig. 2), $a_{k,o}$ is the decomposed sub-band image and l_k^* is the corresponding corrected low-pass luminance image within radial frequency band k. The corrected low-pass luminance image l_k^* is obtained from the original low-pass luminance image l_k by enforcing a cut-off at low luminance levels and an enhancement at high luminance levels to account for the reduction of contrast sensitivity due to the breakdown of Weber's Law for very dark and very bright luminance levels.[21]

The next stage in the model characterizes the masking effect of the HVS, and is also most debated in the literature. While many HVS models account for the nonlinear contrast response of neurons, we only focus on the perceptual tolerance to contrast difference in each frequency band. The visual response in band (k,o) is modeled computationally as

$$r_{k,o}(x,y) = \frac{c_{k,o}^{ref}(x,y) - c_{k,o}^{dst}(x,y)}{IP\left(\left\{\overline{c_{p,q}^{ref}}(x,y)\middle|(p,q)\in adj(k,o)\right\}, CSF(k,o)\right)}, \tag{2}$$

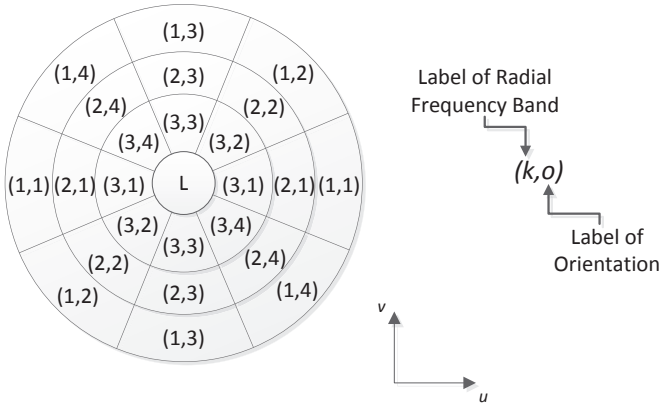

Figure 2. Labels of Decomposed Sub-bands

where $r_{k,o}$ is the visual response in band (k, o), and c^{ref} and c^{dst} are the band-limited contrast of the reference and distorted images, respectively. The function $IP(\cdot)$ defines the contribution of each adjacent band to the sensitivity inhibition of the current band.

The $IP(\cdot)$ function takes as input the local mean contrast of the mask in the adjacent frequency bands and Daly's contrast sensitivity function.[22] It generates an image as its output that depends on the spatial location (x, y). The image $\overline{c^{ref}_{p,q}}(x, y)$ is the average of the local contrast of the mask within a sliding window centered at (x, y) in the band (p, q). The set $adj(k, o)$ consists of the bands that are adjacent to the current band (k, o). For a given frequency band, it includes sub-bands of all orientations in the same radial band. For a given orientation, it includes the frequency bands one octave above and below the current band at the same orientation. As an example, for a sub-band decomposition with 3 levels and 4 orientations, we have

$$adj(k, o) = \{(k-1, o), (k+1, o), (k, 1), (k, 2), (k, 3), (k, 4)\}. \tag{3}$$

In our model, the inhibitory pooling function is defined as

$$\begin{aligned} &IP\left(\left\{\overline{c^{ref}_{p,q}}(x, y) \middle| (p, q) \in adj(k, o)\right\}, CSF(k, o)\right) \\ &\quad = \max\left\{b_c + \sum_{(p,q)\in adj(k,o)} b_{p-k,q-o}\left(\overline{c^{ref}_{p,q}}(x, y)\right)^{\alpha}, \frac{\lambda}{CSF(k, o)}\right\}, \end{aligned} \tag{4}$$

where α is the pointwise nonlinear inhibitory exponent, and b_c and $b_{i,j}$ are linear inhibitory pooling coefficients. Note that the model uses a single set of inhibitory parameters for all bands being inhibited. The linear coefficients are applied to the mask contrasts in adjacent bands based on their locations relative to the current band on the 2-D frequency plane. There are some additional constraints on the linear coefficients:

$$\begin{aligned} b_{i,j} &= b_{i,-j}, \\ b_{i,j} &= b_{i,j\pm O}, \end{aligned} \tag{5}$$

where O is the number of orientations in the linear sub-band decomposition. The first equation comes from a symmetry constraint, meaning that adjacent bands at the same angle relative to the current band on both sides of that band should enforce the same inhibition to the current band. The second equation derives from the circular labeling of sub-band orientations. In the example of Eq. (3), there are 6 linear inhibition parameters: b_c for a constant bias, $b_{0,0}$ for the current band, $b_{0,2}$ for the two orthogonal bands (at ± 90 degrees relative to the

current band), $b_{0,1}$ for the two diagonal bands (at ± 45 degrees relative to the current band), $b_{1,0}$ and $b_{-1,0}$ for radially adjacent bands an octave above and below the current band, respectively.

The max operation is derived from the fact that at very low mask contrast, the masking effect is turned off; and the contrast sensitivity (or detection threshold) at each sub-band simply follows the contrast sensitivity function,[22] which has been investigated intensively for decades.

The final stage of the framework performs a probability summation of the responses across different visual channels:

$$R(x,y) = \left(\sum_{k,o} |r_{k,o}(x,y)|^{\beta} \right)^{\frac{1}{\beta}} \tag{6}$$

where β is usually selected to be between 1.5 and 4. The target visibility map can be generated from $R(x,y)$ via a simple threshold-based decision making process; and the quality map can be built by fitting $R(x,y)$ to subjective scores obtained from psychophysical experiments using a nonlinear transform.

The parameters in our framework include the nonlinear exponent α and the linear coefficients b_c and $b_{i,j}$ in the inhibition pooling function, and β from the probability summation stage. Experimental data is required so as to determine values for the model parameters that are optimized to fit the HVS response. A patch-based psychophysical experiment will be detailed in the next section; and the estimation of optimized parameter values for a general natural texture mask is discussed in Sec. 4.

3. PSYCHOPHYSICAL EXPERIMENT

The goal of the psychophysical experiment is to determine optimized values for the parameters in the inhibitory pooling function, and to verify the model via cross-validation. The basic idea is to find the contrast detection threshold in each visual channel in the presence of a natural texture mask, and then to associate the threshold of detection with the contrast activities of the texture patch in adjacent visual channels.

The nonlinear channel pooling in the visual model gives rise to a nonlinear optimization problem. To overcome the computational difficulty of model fitting, we excite the dominant response in each visual channel individually by applying a 2-D sinusoidal target with impulse frequency content located at the center of each visual sub-band. For example, with a reasonable selection for the value of β, if the visual channel (k^*, o^*) is excited with an impulse excitation in band (k^*, o^*), the response in the particular channel (k^*, o^*) becomes dominant, meaning that $|r_{k^*,o^*}| \gg |r_{k,o}|$ for $\forall (k,o) \neq (k^*, o^*)$; and thus the total visual response can be approximated by the channel response:

$$R(x,y) = \left(\sum_{k,o} |r_{k,o}(x,y)|^{\beta} \right)^{\frac{1}{\beta}} \approx |r_{k^*,o^*}|. \tag{7}$$

This is a very convenient condition that we utilize to simplify optimal parameter estimation in Sec. 4.

3.1 Apparatus and environment

Stimuli are displayed on a 22 in HP L2208w HD monitor (Hewlett-Packard Company, Palo Alto, CA) at a resolution of 28 pixels/cm^2. The display renders a luminance range of $0.4 - 176$cd/m^2. The monitor is characterized using the method described by Arslan[23] so that the digital RGB input can be mapped to CIE XYZ values of the light emitted from the display. The luminance and chromaticity are measured using a colorimeter PR-705 (PhotoResearch, Inc., Chatsworth, CA). All stimuli are viewed in a darkened room at a distance of about 60 cm, which leads to a visual resolution of 30 pixels/degree.

3.2 Stimuli

The set of texture masks used in this work consists of five 128×128 homogeneous color texture images obtained from the MIT Vision Texture Database (http://vismod.media.mit.edu/vismod/imagery/VisionTexture/, See Fig. 3). Although in the current model we don't account for chromaticity masking, which will be part of our future work, we choose textures with relatively neutral color to minimize the influence of chromaticity so that we can still assume the masking effects come primarily from the luminance channel. As is shown later in the paper, it turns out that the model works quite well for the color textures used in the experiment.

Bark *Brick* *Fabric1* *Fabric2* *Peanuts*

Figure 3. Texture masks used in the experiment.

We generate masks of seven levels of contrast from each texture patch. The contrast of each mask is adjusted by adding a controlled local variation to the mean color intensity in each color channel of the patch:

$$\begin{aligned} \hat{R} &= \alpha(R - \mu_R) + \mu_R, \\ \hat{G} &= \alpha(G - \mu_G) + \mu_G, \\ \hat{B} &= \alpha(B - \mu_B) + \mu_B. \end{aligned} \tag{8}$$

where R, G, B and $\hat{R}$, $\hat{G}$, $\hat{B}$ denote the colors of the texture images before and after contrast adjustment, respectively, and α is the scaling factor that controls the contrast. The contrast of the mask texture is computed only in the Y channel of the image using the RMS contrast definition.[20] Following the practice in previous work,[16] we choose the seven levels of RMS contrast to be $0.01, 0.02, \ldots, 0.64$.

The targets applied to the masks are sinusoidal signals in three radial frequency bands one octave apart with four orientations, resulting in 12 different targets for each mask. To generate the stimuli, the target signal is added evenly to the RGB channels of the mask with an adjustable magnitude. For each combination of the masks and targets, seven different thresholds need to be measured for a complete TvC (threshold vs. contrast) curve, which depicts the threshold elevation as a function of the contrast of the mask. Considering that the masking effect in the low mask contrast region is not fully activated, we only measure the threshold of detection in the low mask contrast region (with RMS contrast below 0.08) for half of the stimuli (all texture masks combined with vertical and 45-degree oriented targets) to simplify the phychophysical task. Example stimuli generated from the texture *Brick* at RMS contrast 0.16 combined with sinusoidal targets of different frequencies and orientations are illustrated in Fig. 4.

3.3 Procedures

The thresholds are measured via a yes/no procedure. On each trial, the subjects are asked to view a patch containing mask and target. The initial strength and phase of the target are randomized. The subjects give a response by indicating whether the target is visible or not. A black patch is shown to the subjects for 2 seconds; and the phase of the target is shifted by a random value between two successive trials so as to minimize memory effects. The contrast of the target can be adjusted via α. If the choice is visible, the contrast of the target is decreased; if the choice is invisible, the contrast of the target is increased. The target contrasts are controlled via a QUEST procedure[24] using a Weibull psychometric function[24] parameterized by $\epsilon = 1.15$, $\beta = 3.5$, $\gamma = 0$.

3.4 Subjects

Two expert subjects participated in this experiment; Both are graduate students at Purdue University working in the area of image processing. Each subject made two evaluations for each stimulus separated in time by two days.

3.5 Results and analysis

Figure 5 shows the experiment results in the form of TvC curves, where the just noticeable band-limit contrast difference is depicted as a function of the RMS contrast of the mask. Each curve illustrates the threshold elevation for a particular frequency band, as the contrast of mask changes. As is observed from Fig. 5, at very low mask contrast levels, the thresholds exhibit limited dependency on the mask contrast. This is due to the fact that the masking effect is not fully activated at these mask contrast levels; and the threshold can be described via the CSF,[22] which only depends on the frequency and orientation of the excitation.

When the masking effect is activated, the detection thresholds rise almost linearly with the RMS contrast of the mask on a log-log scale. Moreover, the threshold elevation in each visual channel is a strong function of the type of mask. Textures with finer details (*Fabric1,2*) tend to mask high frequency targets ($k = 1$) more significantly than coarse textures (*Bark, Brick*), while coarse textures put more masking over the middle and low frequency targets ($k = 2, 3$). And textures that exhibit strong directional patterns (e.g. *Bark* exhibits vertically oriented patterns) enforce a stronger mask on targets with similar orientation ($o = 1$). This result provides the rationale for the model of adjacent visual channel inhibition.

4. FITTING THE MODEL TO THE EXPERIMENT RESULT

First, we pool across each patch spatially using an $L2$ norm to get a metric that is independent of spatial position for the contrast difference and mask contrast

$$\begin{aligned} \overline{d_{k,o}} &= \sqrt[2]{\frac{1}{M_{k,o}} \sum_{x,y} \left| c^{ref}_{k,o}(x,y) - c^{def}_{k,o}(x,y) \right|^2}, \\ \overline{c^{m}_{p,q}} &= \sqrt[2]{\frac{1}{M_{p,q}} \sum_{x,y} \left| c^{ref}_{p,q}(x,y) \right|^2}. \end{aligned} \tag{9}$$

Here $M_{k,o}$ is the number of pixels in the sub-band image $a_{k,o}(x, y)$, $\overline{d_{k,o}}$ is the spatially averaged contrast difference in band (k, o); and $\overline{c^{m}_{p,q}}$ is the spatially averaged mask contrast in the adjacent band (p, q).

Without loss of generality, we set the just noticeable response of the model to unity. As was mentioned in the previous section, the band-pass excitation facilitates the parameter estimation by approximating the total visual response with the band-pass response in the excited channel.

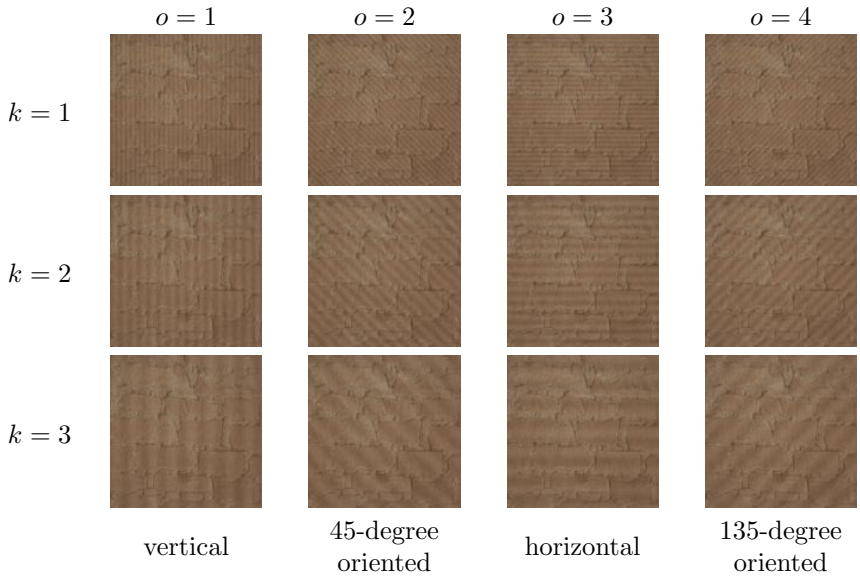

Figure 4. Example stimuli generated from the texture *Brick* at RMS contrast 0.16 combined with sinusoidal targets of different frequencies and orientations.

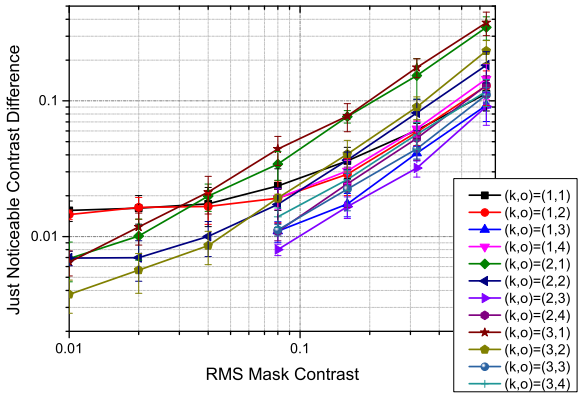

(a) Bark

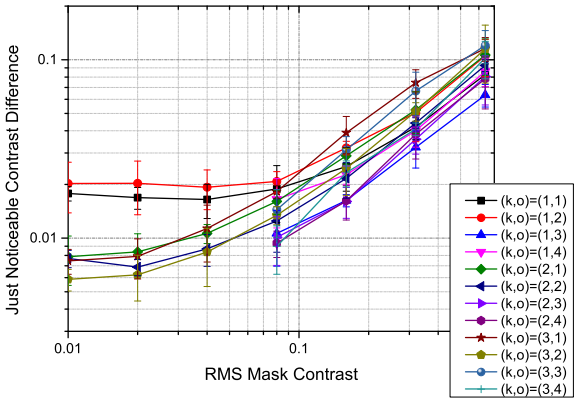

(b) Brick

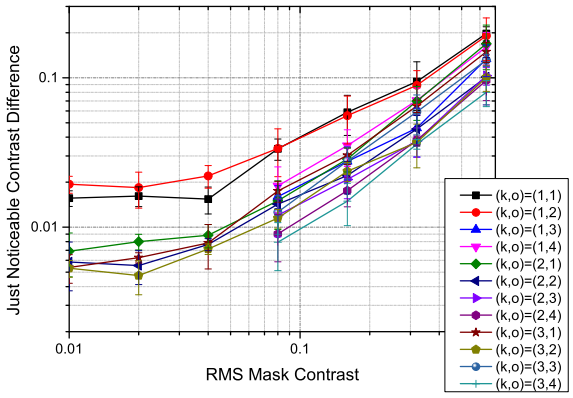

(c) Fabric1

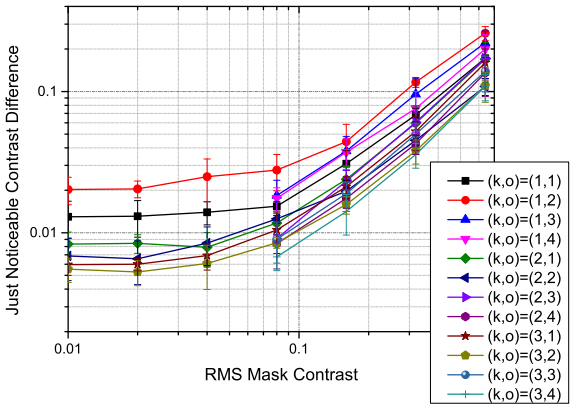

(d) Fabric2

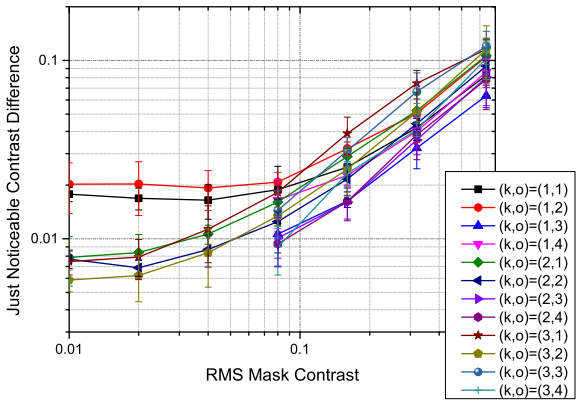

(e) Peanuts

Figure 5. TvC curves obtained from the psychophysical experiment.

Since at low mask contrast region the masking effect has not been fully activated and can be described simply by CSF, we only focus on the masking behavior in the middle and high mask contrast regions (RMS contrast above 0.08). When the masking effect is activated, at the detection threshold for sub-band (k^*, o^*), we have

$$\overline{r_{k^*,o^*}} = \frac{\overline{d_{k^*,o^*}}}{IP\left(\left\{\overline{c^m_{p,q}} \middle| (p,q) \in adj(k^*,o^*)\right\}, CSF(k^*,o^*)\right)} \approx 1. \tag{10}$$

or equivalently,

$$b_c + \sum_{(p,q)\in adj(k^*,o^*)} b_{p-k^*,q-o^*} \overline{c^m_{p,q}}^{\alpha} = \overline{d_{k^*,o^*}}. \tag{11}$$

In other words, with fixed α the task of parameter estimation boils down to a linear regression problem. The value for α is selected by trying different values between 0.5 and 2, and choosing the one resulting in the least fitting error. Following this procedure, optimal value for α is found to be 0.9.

To ensure complete activation of visual masking, experiment data with mask contrast above 0.08 is used for the model training. The training samples include the 60 TvC curves from 12 targets for different radial frequencies and orientations applied to the five texture masks.

Feature selection is done by applying a LASSO penalty[25] to the regression. Figure 6 illustrates the LASSO regression result for choosing the linear inhibition parameters. The horizontal axis shows the penalty λ in log scale; and the vertical axis shows the magnitudes of the linear inhibitory parameters.

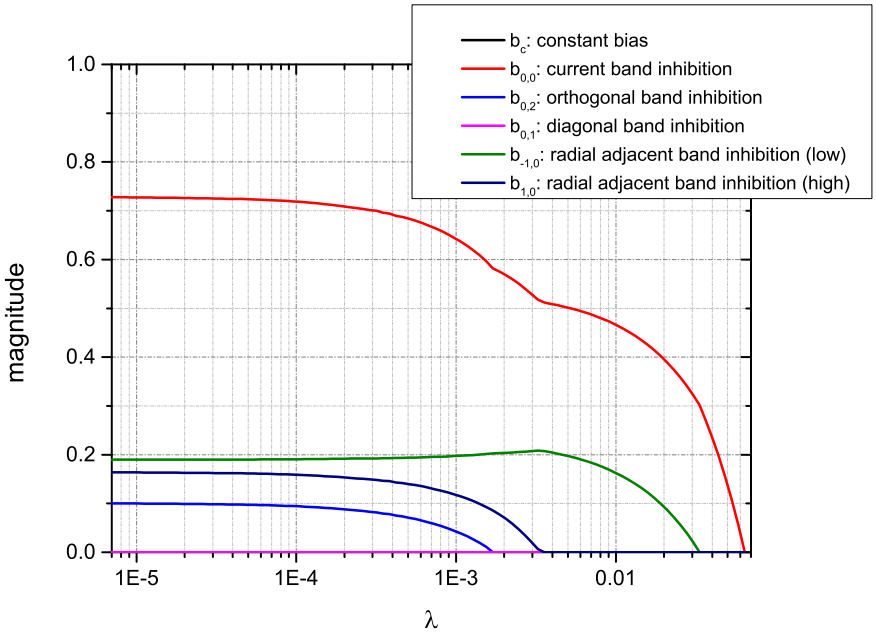

Figure 6. LASSO regression result for the linear inhibitory parameters.

Not surprisingly, the mask contrast in the same band as the excitation plays the most important role in the pattern masking. The next most important component is the mask contrast in the adjacent band one octave below the excited channel, followed by the contrast in the adjacent band an octave above the excited band. The orthogonal band contrast of the mask also makes some contribution to the inhibition. The constant bias b_c and the contrast response in diagonal channels provide negligible contributions to the inhibition. This may be due to the fact that the diagonal components of the mask also excite the center and orthogonal channels, and thus express their contribution in the inhibitory coefficients for center and orthogonal channels. This explains the

psychophysical result in Sec. 3 that textures with a strong pattern in the frequency bands adjacent to that of the target signal place a stronger perceptual mask over the targets.

Cross-validation is performed to evaluate the performance of this model in predicting the detection threshold of each visual channel in the presence of a natural mask. We adopt the leave-one-out strategy, using four of the texture masks as training samples and the one remaining as the testing sample. In other words, 48 TvC curves are used in the training; and 12 are used to test the prediction accuracy. The training is primarily based on the measured thresholds in the middle and high contrast parts of the TvC curve. The prediction in the low mask contrast region is primarily obtained from the classic CSF. The cross-validation result is given in Fig. 7.

Each graph in Fig. 7 illustrates the testing result with one of the texture masks, using the parameters trained on the other four texture patches. Despite the great variation among the texture patterns, the predicted detection thresholds in each visual channel generally correspond quite well with the actual measurement. This cross-validation demonstrates reasonable prediction performance of the model for natural texture masks even with very different mask patterns.

5. CONCLUSION

In this work, we develop a contrast masking model based on adjacent visual channel inhibition. In this model, each visual channel is excited by the contrast difference between the reference and distorted images in that channels and suppressed by the activities of the mask in adjacent channels. A psychophysical experiment is conducted to collect data that reflects the human response to band-pass target excitation in the presence of natural masks. Optimized parameters are obtained by fitting the model to the experiment result. Cross-validation is performed on a set of natural textures with different patterns to demonstrate the model's good performance in predicting the target detection threshold in the presence of natural textures.

REFERENCES

[1] Laparra, V., Munoz-mar, J., and Malo, J., "Divisive normalization image quality metric revisited," *J. Optical Soc. Am. A* **27**, 852–64 (2010).

[2] Watson, A. B. and Solomon, J. A., "Model of visual contrast gain control and pattern masking," *J. Optical Soc. Am. A* **14**, 2379–91 (1997).

[3] Daly, S. J. and Rogowitz, B. E., "Visible differences predictor: an algorithm for the assessment of image fidelity," *Proc. SPIE* **1666**, 2–15 (1992).

[4] Osberger, W., Maeder, A. J., and McLean, D., "A computational model of the human visual system for image quality assessment," *Proc. DICTA'97* **97** (1997).

[5] Teo, P. C. and Heeger, D. J., "Perceptual image distortion," *Proc. ICIP-94* **2**, 982–986 (1994).

[6] Legge, G. E. and Foley, J. M., "Contrast masking in human vision," *J. Optical Soc. Am.* **70**, 1458–71 (1980).

[7] Watson, A. B., Borthwick, R., Taylor, M., Rogowitz, B. E., and Pappas, T. N., "Image quality and entropy masking," *Proc. SPIE* **3016**, 2–12 (1997).

[8] Nadenau, M. J. and Reichei, J., "Image compression related contrast masking measurements," *Proc. SPIE* **3959**, 188–199 (2000).

[9] Masry, M., Chandler, D. M., and Hemami, S. S., "Digital watermarking using local contrast-based texture masking," *Conf. Rec. 37th Asilomar Conf. Signals, Syst. and Comput.* **2**, 1590–1594 (2003).

[10] Wang, Z., Bovik, A. C., Sheikh, H. R., and Simoncelli, E. P., "Image quality assessment: from error visibility to structural similarity," *IEEE Trans. Image Process.* **13**, 600–612 (2004).

[11] Chandler, D. M. and Hemami, S. S., "VSNR: A wavelet-based visual signal-to-noise ratio for natural images," *IEEE Trans. Image Process.* **16**, 2284–98 (2007).

[12] Wang, Z., Simoncelli, E. P., and Bovik, A. C., "Multi-scale structural similarity for image quality assessment," *Conf. Rec. Asilomar Conf. Signals, Syst. and Comput.* **2**, 1398–1402 (2003).

[13] Sheikh, H. R. and Bovik, A. C., "Image information and visual quality," *IEEE Trans. Image Process.* **15**, 430–444 (2006).

[14] Chandler, D. M., "Seven challenges in image quality assessment: past, present, and future research," *ISRN Signal Process.* **2013**, 53 (2013).

[15] Winkler, S., "Visual quality assessment using a contrast gain control model," *1999 IEEE 3th Workshop Multimedia Signal Process.* , 527–532 (1999).
[16] Chandler, D. M., Gaubatz, M. D., and Hemami, S. S., "A patch-based structural masking model with an application to compression," *EURASIP J. Image and Video Process.* **2009** (2009).
[17] Chandler, D. M. and Hemami, S. S., "Effects of natural images on the detectability of simple and compound wavelet subband quantization distortions," *J. Optical Soc. Am. A* **20**, 1164–80 (2003).
[18] Bradley, A. P., "A wavelet visible difference predictor," *IEEE Trans. Image Process.* **8**, 717–730 (1999).
[19] Taylor, C. C., Pizlo, Z., Allebach, J. P., and Bouman, C. A., "Image quality assessment with a Gabor pyramid model of the human visual system," *Proc. SPIE* **3016**, 58–69 (1997).
[20] Peli, E., "Contrast in complex images," *J. Optical Soc. Am. A* **7**, 2032–40 (1990).
[21] Weber, E. H., [*EH Weber on the tactile senses*], Psychology Press (1996).
[22] Daly, S. J., "Application of a noise-adaptive contrast sensitivity function to image data compression," *Optical Eng.* **29**, 977–987 (1990).
[23] Arslan, O., Pizlo, Z., and Allebach, J. P., "CRT calibration techniques for better accuracy including low-luminance colors," *Proc. SPIE* (2003).
[24] Watson, A. and Pelli, D., "QUEST: A bayesian adaptive psychometric method," *Perception & Psychophysics* **33**, 113–120 (1983).
[25] Tibshirani, R., "Regression shrinkage and selection via the LASSO," *J. R. Stat. Soc. Ser. B Stat. Methodol.* **58**, 267–288 (1996).

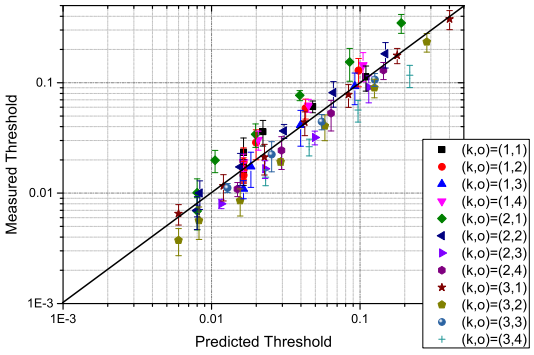

(a) Testing Result with *Bark*, using parameters trained on *Brick*, *Fabric*1, *Fabric*2, *Peanuts*

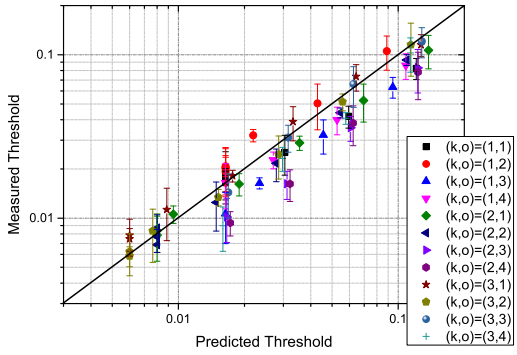

(b) Testing Result with *Brick*, using parameters trained on *Bark*, *Fabric*1, *Fabric*2, *Peanuts*

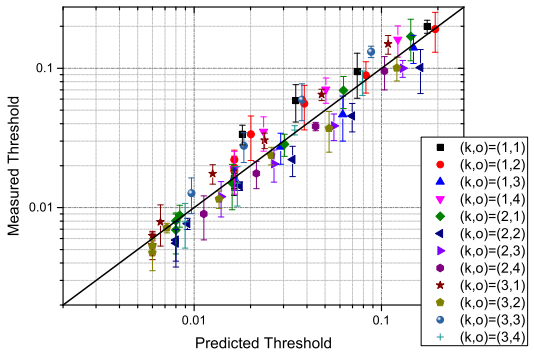

(c) Testing Result with *Fabric*1, using parameters trained on *Bark*, *Brick*, *Fabric*2, *Peanuts*

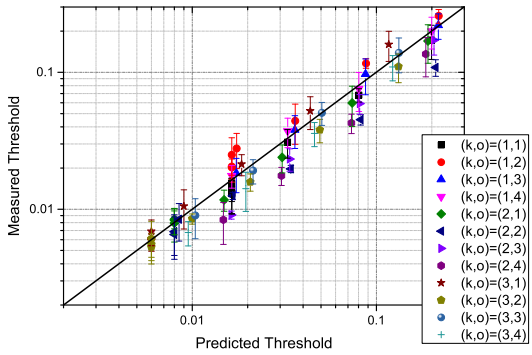

(d) Testing Result with *Fabric*2, using parameters trained on *Bark*, *Brick*, *Fabric*1, *Peanuts*

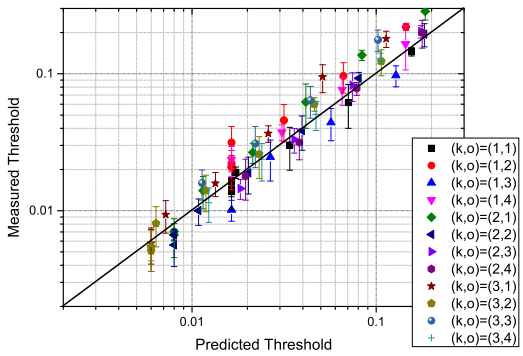

(e) Testing Result with *Peanuts*, using parameters trained on *Bark*, *Brick*, *Fabric*1, *Fabric*2

Figure 7. Cross-validation result of the predicted detection thresholds in the presence of texture masks.